

Markovian Generation Chains in Large Language Models

Mingmeng Geng[†]
ENS-PSL & CNRS-Lattice
mingmeng.geng@ens.psl.eu

Amr Mohamed[†]
MBZUAI & Ecole Polytechnique

Guokan Shang
MBZUAI

Michalis Vazirgiannis
MBZUAI & Ecole Polytechnique

Thierry Poibeau
ENS-PSL & CNRS-Lattice

Abstract

The widespread use of large language models (LLMs) raises an important question: how do texts evolve when they are repeatedly processed by LLMs? In this paper, we define this iterative inference process as *Markovian generation chains*, where each step takes a specific prompt template and the previous output as input, without including any prior memory. In iterative rephrasing and round-trip translation experiments, the output either converges to a small recurrent set or continues to produce novel sentences over a finite horizon. Through sentence-level Markov chain modeling and analysis of simulated data, we show that iterative process can either increase or reduce sentence diversity depending on factors such as the temperature parameter and the initial input sentence. These results offer valuable insights into the dynamics of iterative LLM inference and their implications for multi-agent LLM systems.

1 Introduction

Large language models (LLMs) are used in a wide range of downstream tasks, such as translation and rewriting. As LLM-generated content becomes more prevalent, the likelihood that such content will be iteratively reprocessed increases. This motivates a practical but underexplored question: *how do texts evolve under repeated LLM reprocessing?*

We refer to this process as *Markovian generation chains in LLMs*: the input consists only of a specific prompt template and the output of the previous inference, without including any prior memory. Although such recursive reuse arises naturally in iterative translation and repeated rephrasing workflows (Perez et al., 2025; Mohamed et al., 2025), it lacks a standard formalization and well-defined metrics for characterizing these outcomes.

We treat each *sentence* as the primary unit of analysis and focus on the evolution in the iterative procedure, e.g., quantifying diversity based on how many *distinct sentences* emerge over the repeated process. While LLM outputs are largely determined by the input, the model (Jang et al., 2016) and the hardware (He & Lab, 2025) may also introduce variation. Furthermore, although a one-to-one correspondence cannot be constructed at the token level, it becomes feasible at the sentence level. Therefore, at the sentence level, the iterative reprocessing procedure can be described using a Markov chain, differing from previous work that analyzes a single inference at the token level using Markov chains (Zekri et al., 2024). Markov chains have also been used in other studies on LLMs, such as the reasoning process (Teng et al., 2025).

The accumulation of random perturbations and systematic biases can lead to equilibrium, periodic behavior, divergence, or random walk. The prevalence of these behaviors depends on the model, the decoding configuration, and the seed input sentence; in particular, sampling-based decoding typically increases exploration and prolongs pre-recurrence phases. Figure 1 provides an illustration of these behaviors under greedy versus sampling-based decoding.

[†]Equal contribution.

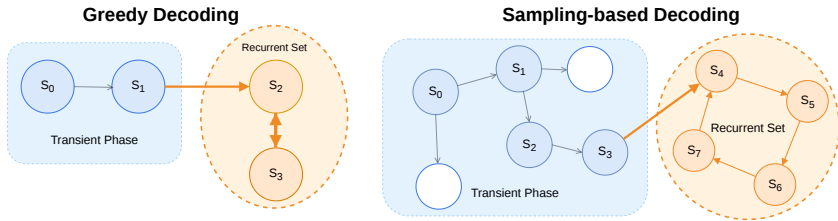


Figure 1: Illustration of iterative LLM reprocessing (*Markovian generation chains*). Each node denotes the output after iteration i . Under **greedy decoding**, chains typically enter fixed points or short cycles, limiting sentence-level diversity. Under **sampling-based decoding**, stochasticity may yield longer transients and more distinct outputs

These iterative dynamics matter beyond controlled settings because LLM-mediated text can propagate through downstream communication and decision pipelines. Prior work suggests that LLMs may reshape collective intelligence (Burton et al., 2024), and that repeated generation can introduce information distortion even when prompts request meaning preservation (Mohamed et al., 2025). In our experiments, text produced by an LLM via paraphrasing or translation is recursively reused as input, approximating multi-step and multi-user reprocessing workflows in the real world. The sentence-level framing supports a natural mapping between an input sentence and the set of plausible output sentences, and it could be extended to paragraph-level simulations as an ablation.

2 Related Work

Model collapse and iterative generation. A growing line of work studies *model collapse*, where iteratively training on synthetic data can degrade coverage of the underlying data distribution (Shumailov et al., 2024; Guo et al., 2023). Follow-up studies analyze when collapse arises and propose mitigations such as mixing real and synthetic data or other data curation strategies (Gerstgrasser et al., 2024; Seddik et al., 2024), with broader concerns about downstream “knowledge collapse” in information ecosystems (Peterson, 2025; Wright et al., 2025). Repeated LLM use can also form multi-step transformation chains (e.g., iterated paraphrasing or round-trip translation) that accumulate changes across calls, with observed distortion (Perez et al., 2025; Mohamed et al., 2025).

Sampling and diversity in LLM-generated content. Sampling methods derived from the softmax distribution, including top- k (Fan et al., 2018), top- p (Holtzman et al., 2019), and temperature-based sampling or logit suppression (Chung et al., 2023), induce controlled randomness in generation, despite known limitations of softmax-based sampling in certain regimes (Chang & McCallum, 2022). Moreover, architectural and distributional constraints impose statistical regularities on outputs (Mikhaylovskiy, 2025). A substantial body of work studies stylistic and diversity differences between LLM-generated and human-written text (Muñoz-Ortiz et al., 2024). Several studies suggest that LLM-assisted generation can reduce downstream diversity, including in creative settings (Padmakumar & He, 2023; Xu et al., 2025; Jiang et al., 2025). Most evaluations of LLM-generated content emphasize token-, phrase-, or corpus-level statistics (Chung et al., 2023; Guo et al., 2024; Smith et al., 2025), sentence-level variation is a natural granularity for iterative rewriting and translation pipelines, providing a transparent and interpretable complement to existing metrics.

Language change and convergence in human–LLM interaction. Our work also relates to research on language change and cultural transmission (Lieberman et al., 2007; Kirby et al., 2007; Griffiths & Kalish, 2007; Hamilton et al., 2016) and to studies of machine-mediated communication (Brinkmann et al., 2023; Arnon & Kirby, 2024). In interaction settings, LLMs adapt to conversational partners (Kandra et al., 2025; Blevins et al., 2025). Users may learn and converge toward model language patterns over time (Yakura et al., 2024; Geng et al., 2025), and even more complex interaction dynamics have also been observed (Geng & Trotta, 2025). We contribute an inference-time mechanism, iterative reprocessing under a fixed prompting setup, that provides a controlled lens on repeated reuse in these settings.

3 Methodology

This section formalizes iterative processes as *Markovian generation chains* and introduces the tools used to analyze the empirical regimes in our experiments.

3.1 Iterative reprocessing as a Markovian generation chain

Let $s^{(0)}$ denote an initial *sentence*. Fix (i) a model M , (ii) a prompt template ρ , and (iii) a decoding configuration d (e.g., greedy decoding, or sampling-based decoding with specified temperature/top- p). One step of iterative reprocessing defines a stochastic transformation operator $\mathcal{T}_{M,\rho,d}$ that maps the text-unit surface string to a distribution over surface strings:

$$s^{(t+1)} \sim \mathcal{T}_{M,\rho,d}(\cdot | s^{(t)}), \quad t = 0, 1, \dots, T-1. \quad (1)$$

Equivalently, $\mathcal{T}_{M,\rho,d}$ defines a time-homogeneous Markov kernel $P_{M,\rho,d}(s' | s)$ over sentences. We restrict the state space to single-sentence strings by requiring each iteration to output exactly one sentence. Further details are explained in Appendix A.

Operational Markovian assumption. Iterations are independent model calls conditioned only on ρ and $s^{(t)}$; no history, memory, or latent state is carried between steps. Thus $\{s^{(t)}\}_{t=0}^T$ is Markovian, with any system nondeterminism absorbed into $P_{M,\rho,d}$.

Structured operators via composition. A single iteration can be written as a composition of prompted calls. For round-trip translation with bridge language ℓ , one iteration composes two translations ($\text{EN} \rightarrow \ell$ then $\ell \rightarrow \text{EN}$). Let $\mathcal{T}_{M,\rho,d}^{\text{EN} \rightarrow \ell}$ and $\mathcal{T}_{M,\rho,d}^{\ell \rightarrow \text{EN}}$ denote the induced operators for each direction under the same fixed setup. The resulting EN-to-EN two-step operator is

$$\mathcal{T}_{M,\rho,d}^{\text{EN} \rightarrow \ell \rightarrow \text{EN}} := \mathcal{T}_{M,\rho,d}^{\ell \rightarrow \text{EN}} \circ \mathcal{T}_{M,\rho,d}^{\text{EN} \rightarrow \ell}, \quad (2)$$

which induces a Markov chain on English sentences. At the kernel level, this composition corresponds to the standard product of Markov kernels:

$$P_{M,\rho,d}^{\text{EN} \rightarrow \ell \rightarrow \text{EN}}(s' | s) = \sum_{u \in \mathcal{S}_\ell} P_{M,\rho,d}^{\ell \rightarrow \text{EN}}(s' | u) P_{M,\rho,d}^{\text{EN} \rightarrow \ell}(u | s), \quad (3)$$

where \mathcal{S}_ℓ denotes the (conceptual) state space of sentences in language ℓ .

3.2 Sentence-level Markov chain formulation

We model iterative reprocessing at the *sentence* level, treating sentence strings as discrete states and the prompted model as a transition operator. For conceptual clarity, we consider finite (but extremely large) state spaces.

State spaces. For translation between languages l_A and l_B , let $\mathcal{S}_A = \{a_1, \dots, a_m\}$, $\mathcal{S}_B = \{b_1, \dots, b_n\}$. For rephrasing, the chain remains within a single language, i.e., $\mathcal{S}_A \rightarrow \mathcal{S}_A$.

Transition matrices. Fix (M, ρ, d) . For translation from l_A to l_B , define the sentence-level transition matrix

$$[\mathbf{P}_{M,\rho,d}^{A \rightarrow B}]_{ij} := \Pr(b_j | a_i; M, \rho, d) = P_{M,\rho,d}^{A \rightarrow B}(b_j | a_i). \quad (4)$$

For round-trip translation $l_A \rightarrow l_B \rightarrow l_A$, the induced within- \mathcal{S}_A transition matrix is the product

$$\mathbf{P}_{M,\rho,d}^{A \rightarrow B \rightarrow A} = \mathbf{P}_{M,\rho,d}^{A \rightarrow B} \mathbf{P}_{M,\rho,d}^{B \rightarrow A}, \quad (5)$$

mirroring the kernel composition in Eq. (3). If $X^{(0)}$ denotes an initial distribution over \mathcal{S}_A represented as a row vector, then after n iterations

$$X^{(n)} = X^{(0)} \left(\mathbf{P}_{M,\rho,d}^{A \rightarrow B \rightarrow A} \right)^n. \quad (6)$$

For iterative rephrasing, we use the analogous within-language matrix $\mathbf{P}_{M,\rho,d}$ on \mathcal{S}_A .

3.3 Regimes under iteration: recurrent classes and transients

Empirically, iterative reprocessing exhibits two finite-horizon behaviors: (i) *early exact recurrence* (a fixed point or short cycle) and (ii) *long pre-recurrence phases* (continued production of novel surface forms within the iteration budget). We characterize these regimes using finite-horizon recurrence statistics computed on exact string equality.

Asymptotic structure (conceptual). For a finite state space, \mathbf{P} can be permuted into the standard block form with recurrent classes $\{C_i\}$ and a transient block \mathbf{P}_{tr} (Eq. 7); early recurrence corresponds to fast entry into a small recurrent class, while long pre-recurrence corresponds to trajectories that remain in transient regions over the finite horizon.

$$\mathbf{P} = \begin{bmatrix} \mathbf{P}_1 & \mathbf{0} & \cdots & \mathbf{0} & \mathbf{0} \\ \mathbf{0} & \mathbf{P}_2 & \cdots & \mathbf{0} & \mathbf{0} \\ \vdots & \vdots & \ddots & \vdots & \vdots \\ \mathbf{0} & \mathbf{0} & \cdots & \mathbf{P}_c & \mathbf{0} \\ \mathbf{Q}_1 & \mathbf{Q}_2 & \cdots & \mathbf{Q}_c & \mathbf{P}_{\text{tr}} \end{bmatrix}, \quad (7)$$

where \mathbf{P}_i governs motion within C_i , \mathbf{Q}_i captures transitions from transient states into C_i , and \mathbf{P}_{tr} governs transient-to-transient motion. In extremely large sentence state spaces, these sets are primarily a conceptual aid: empirical trajectories are finite, and the chain may not exhibit observable recurrence within the chosen horizon.

Finite-horizon recurrence statistics. We treat “exact” equality as literal string equality on model outputs. Given a trajectory $\{s^{(t)}\}_{t=0}^T$, the first recurrence time is

$$\tau_T = \min\{t \in \{1, \dots, T\} : \exists j < t \text{ such that } s^{(t)} = s^{(j)}\}, \quad (8)$$

with $\tau_T = T + 1$ if no exact repeat occurs within the horizon. Small τ_T corresponds to early entry into a fixed point or short cycle; large τ_T (or $T + 1$) corresponds to a long pre-recurrence phase within T steps.

Effect of decoding on pre-recurrence behavior. Decoding controls inside d (e.g., temperature/top- p) affect \mathbf{P} by redistributing transition mass. Sampling-based decoding typically increases probability assigned to lower-ranked continuations, enlarging the set of accessible next-step realizations and thereby increasing τ_T on average, i.e., prolonging pre-recurrence phases relative to greedy decoding.

3.4 Information-theoretic tools for iterative reprocessing

We record three standard properties of the induced kernel \mathbf{P} —entropy behavior, Kullback-Leibler (KL) contraction, and mixture bounds—that help interpret diversity and stabilization under iteration.

Entropy under doubly stochastic kernels. Let X be a distribution over sentences and \mathbf{P} a row-stochastic transition matrix (the kernel induced by (M, ρ, d)). The sentence entropy is

$$H(X) = - \sum_s X(s) \log X(s). \quad (9)$$

If \mathbf{P} is doubly stochastic, then $H(X\mathbf{P}) \geq H(X)$; otherwise (as for prompted LLM kernels) entropy may increase or decrease depending on X and \mathbf{P} .

Data processing and KL contraction. For distributions X, Y over sentences, KL divergence contracts under a stochastic matrix:

$$D_{\text{KL}}(X\mathbf{P} \parallel Y\mathbf{P}) \leq D_{\text{KL}}(X \parallel Y), \quad (10)$$

Proof in Appendix B. If π is stationary ($\pi\mathbf{P} = \pi$), then $D_{\text{KL}}(X\mathbf{P}^n \parallel \pi)$ is non-increasing in n , formalizing stabilization under repeated application of the same kernel.

Mixtures of original and reprocessed text. To reflect settings where original and model-processed text coexist, consider the mixture $Y = bX + (1 - b)XP$ for $b \in [0, 1]$. Then

$$bH(X) + (1 - b)H(XP) \leq H(Y) \leq bH(X) + (1 - b)H(XP) + h(b), \quad (11)$$

where $h(b) = -b \log b - (1 - b) \log(1 - b)$ is the binary entropy. Thus, mixing bounds the uncertainty of the combined distribution while still allowing iteration to increase or decrease entropy depending on the induced kernel.

3.5 Measurement and evaluations

We used the following methods for measurement and evaluation:

- *Distinct-sentence count:* $U = \left| \{c(s^{(t)}) : 0 \leq t \leq T\} \right|$.
- *First recurrence time:* defined in Eq. 8.
- *Drift:* METEOR (Banerjee & Lavie, 2005), ROUGE-1 (Lin, 2004), BLEU (Papineni et al., 2002), and TF-IDF cosine (2–4 grams), computed stepwise ($s^{(t)}$ vs. $s^{(t-1)}$) and cumulative ($s^{(t)}$ vs. $s^{(0)}$).
- *Input sensitivity:* correlation of seed length with U (Pearson r and linear regression).

4 Experimental Setup

Data We use three corpora spanning distinct domains: *BookSum* (Kryściński et al., 2022), *ScriptBase-alpha* (Gorinski & Lapata, 2015), and *(BBC) News2024* (Li et al., 2024). From each dataset, we randomly sample 150 documents and extract the first sentence as the seed $s^{(0)}$.

Models and baselines. We evaluate instruction-tuned open-weight models: *Mistral-7B-Instruct* (Jiang et al., 2023), *Llama-3.1-8B-Instruct* (Dubey et al., 2024), and *Qwen2.5-7B-Instruct* (Yang et al., 2024). We also include *GPT-4o-mini* (Hurst et al., 2024) via API. For round-trip translation, we compare prompted LLM translation to *Google Translate (v3)* (API), a near-deterministic production MT baseline for fixed inputs.

Decoding configurations and prompts. We compare two decoding regimes. Under **greedy decoding**, tokens are selected by argmax at each step, close to a deterministic mapping. Under **sampling-based decoding**, we sample with fixed hyperparameters for comparability (unless otherwise stated, $\tau = 0.7$, $\text{top-}p = 0.9$). When the stack exposes an explicit random seed, we fix it per chain; otherwise (e.g., APIs) we treat each chain as a stochastic realization and aggregate over many runs. We use ρ_{reph} for rephrasing and ρ_{tr} for each translation direction. Full templates (including alternation variants) are in Appendix C.

5 Results

5.1 Main Results and Findings

Table 1 provides an illustrative greedy-decoding trajectory and Figure 2 reports sentence-level diversity over $T=50$ iterations across datasets and models. Under greedy decoding, trajectories typically enter small recurrent sets (fixed points or short cycles) after few steps, yielding repeated surface strings or short alternations among near-paraphrases. The observed cycle structure and lexical realizations vary by model, indicating model-specific attractors under a fixed prompting setup. For sampling-based decoding, trajectories exhibit longer pre-recurrence phases and a non-trivial fraction of chains show no exact repetition within $T=50$ (Appendix Table 3). Across all datasets, greedy decoding produces substantially fewer unique paraphrases, consistent with rapid entry into recurrent behavior. Sampling yields markedly larger support sizes with substantial heterogeneity across models and domains, suggesting that both the induced kernel (model/decoding) and the seed distribution modulate time-to-recurrence within the finite horizon.

Round	Qwen2.5-7B-Instruct	Llama-3.1-8B-Instruct
0	We <i>begin</i> with a prologue.	We <i>begin</i> with a prologue.
1	We start with a prologue.	The story commences with a prologue.
2	We <i>begin</i> with a prologue.	<u>The narrative</u> <i>begins</i> with a prologue.
3	We start with a prologue.	The story commences with a prologue.
4	We <i>begin</i> with a prologue.	<u>The narrative</u> <i>begins</i> with a prologue.
5	We start with a prologue.	The story commences with a prologue.
6	We <i>begin</i> with a prologue.	<u>The narrative</u> <i>begins</i> with a prologue.

Table 1: Illustrative greedy-decoding trajectories under iterative rephrasing. Qwen2.5-7B enters a 2-cycle after one step, while Llama-3.1-8B alternates between two near-paraphrases with different lexical realizations.

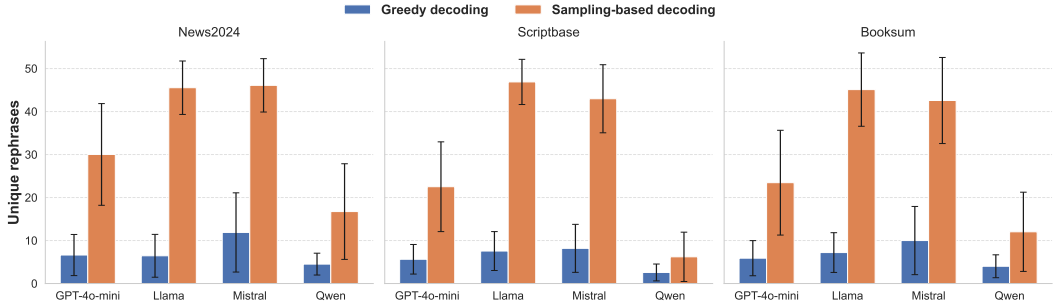


Figure 2: Average number of unique paraphrases generated over 50 iterative rephrasings across three datasets, comparing four instruction-tuned LLMs: GPT-4o-mini, Llama-3.1-8B, Mistral-7B, and Qwen-2.5-7B. Results are shown for greedy decoding (orange) and sampling-based decoding (purple). Error bars represent one standard deviation.

To characterize local dynamics along trajectories, we compute METEOR, ROUGE-1, and BLEU between successive iterations ($s^{(t)}$ vs. $s^{(t-1)}$). Under greedy decoding, these stepwise similarity scores rapidly plateau (Figure 3; Appendix Figures 8 and 9), consistent with confinement to a small recurrent set rather than continued exploration. Differences in plateau levels across models reflect variation in the lexical distance between recurrent paraphrase variants despite comparable semantic content.

5.2 Parameters and Inputs

The behavior of iterative reprocessing depends on both the *decoding configuration* and the *initial input*. Increasing the temperature generally flattens the distribution and increases the probability of selecting lower-ranked tokens, thereby expanding the set of plausible continuations. Supplementary results in Appendix Figures 10–12 indicate that higher-temperature settings tend to delay or prevent rapid entry into small recurrent sets, yielding longer transients with fewer exact repetitions.

The initial input affects the size of the accessible paraphrastic neighborhood and thus the diversity observed along an iterative chain. Table 4 reports the association between seed length (words) and sentence-level diversity (the number of distinct outputs over $T = 50$ iterations) across models, decoding regimes, and datasets. Correlations are generally positive but heterogeneous: sampling often amplifies the effect (notably on BOOKSUM and NEWS2024), while SCRIPTBASE is weaker or inconsistent. Full correlation and regression results are given in Appendix D (Table 6).

Model (Decoding)	BookSum	ScriptBase	News2024
Llama (greedy)	0.17	-0.17	0.19
Llama (sampling)	0.17	0.03	0.11
Mistral (greedy)	0.32	0.07	0.11
Mistral (sampling)	0.44	-0.02	0.20
Qwen (greedy)	0.35	0.09	0.20
Qwen (sampling)	0.49	0.16	0.37
GPT (greedy)	0.48	0.10	0.37
GPT (sampling)	0.64	0.23	0.39

Figure 4: Pearson correlation r between seed length (words) and the number of distinct outputs over $T = 50$ iterations.

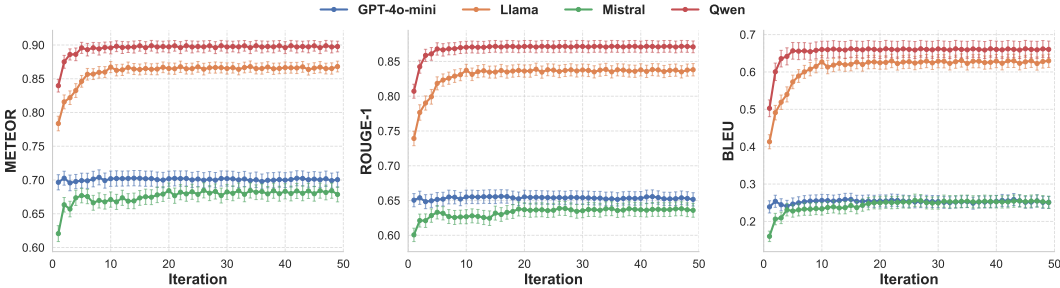


Figure 3: Evolution of text similarity metrics across 50 rephrasing iterations for the BookSum dataset using greedy decoding. Each iteration compares the current rephrased text against the previous iteration’s text as reference.

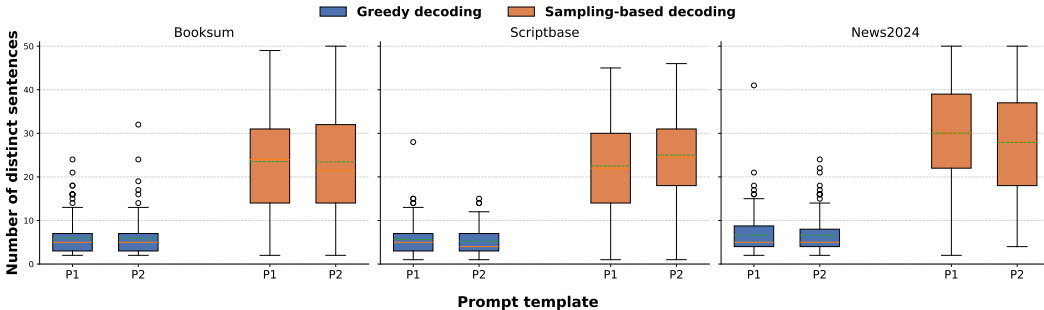


Figure 5: Number of distinct sentences produced over 50 iterative rephrasings with *GPT-4o-mini* under different settings. P1 and P2 correspond to Listings 1 and 2 in the Appendix. Boxes denote the interquartile range, and the center line indicates the median.

5.3 Ablations

We perform a set of ablation studies to evaluate the robustness of the observed iterative regimes and to identify which elements of the chain specification most strongly affect recurrence and output diversity. Specifically, we vary: (i) the prompt template, (ii) prompt heterogeneity across iterations, (iii) the granularity of the input unit (sentences vs. paragraphs), and (iv) the task instantiation via round-trip translation.

5.3.1 Sensitivity to prompt specification and prompt heterogeneity

We first assess the sensitivity of iterative rephrasing dynamics to the prompt template. Using *GPT-4o-mini* as a representative model, we compare two prompt variants (P1 and P2; Listings 1 and 2). As shown in Figure 5, the decoding regime is the primary driver within this prompt range: sampling-based decoding consistently yields a substantially larger number of distinct sentence realizations than greedy decoding, whereas the prompt variation induces comparatively smaller changes. For the prompts considered here, the induced operator is not altered sufficiently to dominate recurrence behavior largely determined by decoding.

To better approximate heterogeneous real-world pipelines, we next introduce prompt heterogeneity across iterations by alternating prompts. This setting remains *Markovian* at the sentence level, but the kernel becomes *time-inhomogeneous*: iteration t uses $P_{M,\rho_t,d}^{(t)}$ rather than a single fixed $P_{M,\rho,d}$. Equivalently, the process can be cast as a time-homogeneous Markov chain on an augmented state space (s, k) where k indexes the active prompt (or prompt schedule). Figure 6 shows that prompt alternation increases the number of distinct outputs relative to a single fixed prompt under the same sampling-based configuration, but does not eliminate exact recurrences: some sentences still reappear across iterations. Round-trip translation can be interpreted as a structured instance of such heterogeneity, since each iteration composes distinct directional mappings ($EN \rightarrow \ell$ and $\ell \rightarrow EN$).

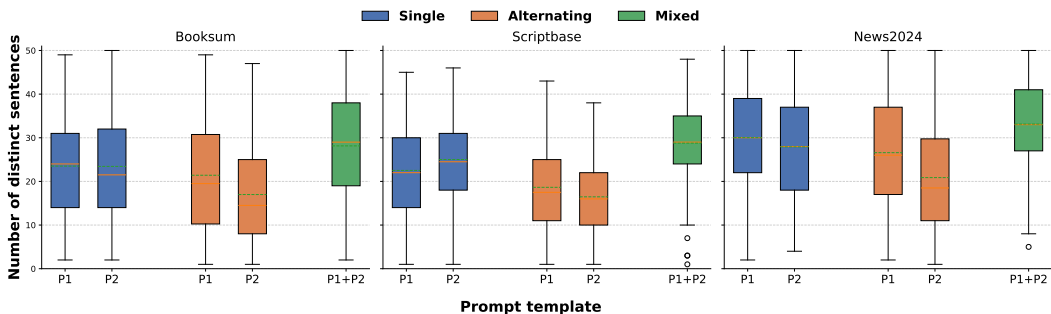


Figure 6: Prompt heterogeneity across iterations (*GPT-4o-mini*, sampling-based decoding). We compare a single fixed prompt against alternating prompts, and a mixed variant constructed from prompt halves.

Sentence	Frequency
Hooray for best friends!	50
I don't think so.	50
You're the ones being banished!"	50
Sue now has two children and is expecting a third.	46
Suddenly, the ghost appears.	41
Jo continues to write short romantic stories for the newspaper while secretly working on a novel.	34
Just as she is about to leave, the Westons arrive in their carriage.	33
Cunegonde resists the advances of both men.	32
They have several children, with Charlotte being the eldest; she is practical, sensible, and intelligent.	32
Madame Defarge passes by and acknowledges them with a nod.	31

Table 2: Highest recurrence frequency observed sentences within the 50-iteration paragraph-level runs (*GPT-4o-mini*, sampling-based decoding, prompt P1) on 150 BookSum paragraphs.

5.3.2 Beyond single sentences: paragraph-level iterative reprocessing

Our primary experiments model the chain state at the sentence level. To examine whether analogous recurrence phenomena persist at larger granularities, we additionally run paragraph-level simulations on 450 paragraph seeds (150 per dataset), using *GPT-4o-mini* with temperature 0.7 and top- p 0.9 for $T = 50$ transitions. Exact recurrence at the paragraph level—i.e., verbatim repetition of the full multi-sentence input—is uncommon within this horizon. However, recurrence remains pronounced at the sentence level: when we segment each paragraph output into sentences, individual sentence forms can reappear frequently across iterations, indicating that local attractor-like behavior can persist even when the state comprises multiple sentences.

To quantify exploration at this granularity, we compute a *normalized diversity ratio*: the number of distinct sentence realizations observed over the iterative trajectory divided by the number of sentences in the original paragraph. Over 50 iterations, this ratio is 26.7 for BookSum, 19.7 for ScriptBase-alpha, and 24.2 for News2024, indicating that iterative paragraph-level reprocessing can generate substantial sentence-level variation even when full-paragraph exact recurrence is rare.

5.3.3 Round-trip translation and comparison to a production MT service

We additionally instantiate iterative reprocessing through round-trip translation ($EN \rightarrow \ell \rightarrow EN$). Appendix Tables 4 and 5 provide qualitative examples of two representative finite-horizon behaviors: early entry into a fixed point and oscillation among a small set of closely related variants.

We evaluate multiple bridge languages and compare sampling-based LLM translation with *Google Translate (v3)* as a production machine translation service baseline. Figure 7 reports distinct-sentence counts under iterated round-trip translation for *GPT-4o-mini* and *Google Translate (v3)*. Unlike prompted LLM translation, which can exhibit substantial stochastic variation under sampling-based decoding, production MT services tend to behave nearly

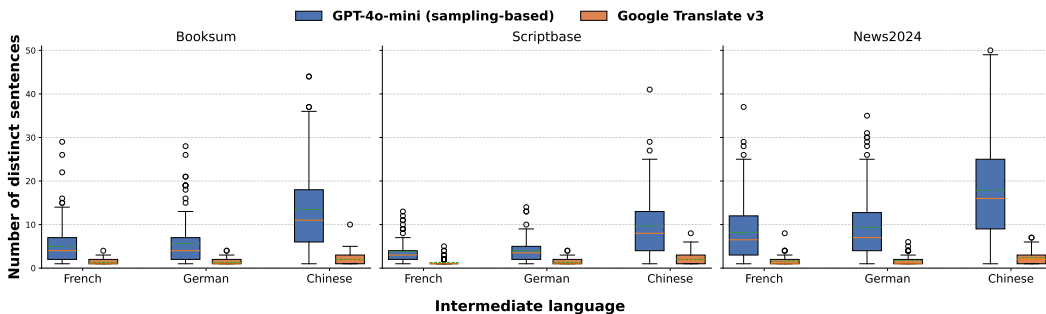


Figure 7: Distinct-sentence counts under iterated round-trip translation for *GPT-4o-mini* (sampling-based decoding) and *Google Translate (v3)*.

deterministically for fixed inputs. These results highlight that prompted LLM translation can induce substantially stronger surface-form variability under iterative reuse than a production MT service, even under a nominal meaning-preservation objective.

5.4 Distinction from training-time model collapse

Shumailov et al. (2024) describe *model collapse* as a training-time phenomenon in which repeated optimization on model-generated data can reduce coverage of the original data distribution. Subsequent analyses argue that the severity of this effect depends on strong assumptions and that it may be attenuated in more realistic training settings (Schaeffer et al., 2025). Our setting is mechanistically distinct: we investigate *inference-time* recursion under a fixed model, prompt, and decoding configuration, where an induced transformation operator is applied iteratively without any parameter updates.

Consequently, the behaviors we observe—including rapid convergence to fixed points or short cycles under greedy decoding and longer transients with sustained production of distinct realizations under sampling-based decoding—are attributable to properties of the induced transition kernel rather than to distributional contraction driven by learning. Moreover, at the sentence level, iterative reprocessing can preserve or even increase the diversity for certain inputs, in contrast to the diversity degradation typically emphasized in training-time collapse accounts. These differences motivate the use of separate terminology and analytical tools for iterative inference dynamics, as formalized in our Markovian generation chain framework.

6 Discussions and Conclusions

LLMs are progressively integrated into text-processing pipelines, where their outputs can be fed into subsequent steps, either within a single workflow or reused across users. Many researchers are interested in exploring the differences between single-turn and multi-turn interactions in LLMs (Li et al., 2025; Laban et al., 2025; Huang et al., 2026), whereas the scenarios considered in our paper can be regarded as multi-single-turn.

LLMs are frequently applied to tasks such as translation and rewriting. Repeated inference-time reprocessing is mechanistically distinct from training-time model-collapse phenomena: the dynamics we study arise from iterating transformation operators rather than from optimizing model parameters on synthetic data. At the same time, sentence diversity does not imply semantic fidelity, as iterative reprocessing can introduce cumulative drift even under meaning-preserving prompts. The behavior of LLMs in a wider range of scenarios also requires further study.

The *Markovian generation chains* we define naturally arise in the real world, for instance through interactions among different LLM agents. Our Markov-chain framing provides a compact way to describe these phenomena and connect them to standard properties of stochastic operators (e.g., contraction of divergences under repeated application of a

fixed kernel). This clear and direct method of explanation can help us broadly understand the simulation results. Therefore, the results of this paper also provide insights into the development and use of LLMs.

Acknowledgments

This work benefited from funding from the French State, managed by the Agence Nationale de la Recherche, under the France 2030 program (grant reference ANR-23-IACL-0008). This research also received support from the ENS-PSL BeYs Chair in Data Science and Cybersecurity. We appreciate the thoughtful conversations and valuable suggestions from Gibbs Nwemadji.

References

- Inbal Arnon and Simon Kirby. Cultural evolution creates the statistical structure of language. *Scientific Reports*, 14(1):5255, 2024.
- Satanjeev Banerjee and Alon Lavie. Meteor: An automatic metric for mt evaluation with improved correlation with human judgments. In *Proceedings of the acl workshop on intrinsic and extrinsic evaluation measures for machine translation and/or summarization*, pp. 65–72, 2005.
- Terra Blevins, Susanne Schmalwieser, and Benjamin Roth. Do language models accommodate their users? a study of linguistic convergence. *arXiv preprint arXiv:2508.03276*, 2025.
- Levin Brinkmann, Fabian Baumann, Jean-François Bonnefon, Maxime Derex, Thomas F Müller, Anne-Marie Nussberger, Agnieszka Czaplicka, Alberto Acerbi, Thomas L Griffiths, Joseph Henrich, et al. Machine culture. *Nature Human Behaviour*, 7(11):1855–1868, 2023.
- Jason W Burton, Ezequiel Lopez-Lopez, Shahar Hechtlinger, Zoe Rahwan, Samuel Aeschbach, Michiel A Bakker, Joshua A Becker, Aleks Berditchevskaia, Julian Berger, Levin Brinkmann, et al. How large language models can reshape collective intelligence. *Nature human behaviour*, 8(9):1643–1655, 2024.
- Haw-Shiuan Chang and Andrew McCallum. Softmax bottleneck makes language models unable to represent multi-mode word distributions. In *Proceedings of the 60th Annual Meeting of the Association for Computational Linguistics*, volume 1, 2022.
- John Joon Young Chung, Ece Kamar, and Saleema Amershi. Increasing diversity while maintaining accuracy: Text data generation with large language models and human interventions. *arXiv preprint arXiv:2306.04140*, 2023.
- Abhimanyu Dubey, Abhinav Jauhri, Abhinav Pandey, Abhishek Kadian, Ahmad Al-Dahle, Aiesha Letman, Akhil Mathur, Alan Schelten, Amy Yang, Angela Fan, et al. The llama 3 herd of models. *arXiv e-prints*, pp. arXiv–2407, 2024.
- Angela Fan, Mike Lewis, and Yann Dauphin. Hierarchical neural story generation. *arXiv preprint arXiv:1805.04833*, 2018.
- Mingmeng Geng and Roberto Trotta. Human-llm coevolution: Evidence from academic writing. In *Findings of the Association for Computational Linguistics: ACL 2025*, pp. 12689–12696, 2025.
- Mingmeng Geng, Caixi Chen, Yanru Wu, Yao Wan, Pan Zhou, and Dongping Chen. The impact of large language models in academia: from writing to speaking. In *Findings of the Association for Computational Linguistics: ACL 2025*, pp. 19303–19319, 2025.
- Matthias Gerstgrasser, Rylan Schaeffer, Apratim Dey, Rafael Rafailov, Henry Sleight, John Hughes, Tomasz Korbak, Rajashree Agrawal, Dhruv Pai, Andrey Gromov, et al. Is model collapse inevitable? breaking the curse of recursion by accumulating real and synthetic data. *arXiv preprint arXiv:2404.01413*, 2024.

- Fabian Gloeckle, Badr Youbi Idrissi, Baptiste Rozière, David Lopez-Paz, and Gabriel Synnaeve. Better & faster large language models via multi-token prediction. *arXiv preprint arXiv:2404.19737*, 2024.
- Philip Gorinski and Mirella Lapata. Movie script summarization as graph-based scene extraction. In *Proceedings of the 2015 Conference of the North American Chapter of the Association for Computational Linguistics: Human Language Technologies*, pp. 1066–1076, 2015.
- Thomas L Griffiths and Michael L Kalish. Language evolution by iterated learning with bayesian agents. *Cognitive science*, 31(3):441–480, 2007.
- Yanzhu Guo, Guokan Shang, Michalis Vazirgiannis, and Chloé Clavel. The curious decline of linguistic diversity: Training language models on synthetic text. *arXiv preprint arXiv:2311.09807*, 2023.
- Yanzhu Guo, Guokan Shang, and Chloé Clavel. Benchmarking linguistic diversity of large language models. *arXiv preprint arXiv:2412.10271*, 2024.
- William L Hamilton, Jure Leskovec, and Dan Jurafsky. Diachronic word embeddings reveal statistical laws of semantic change. *arXiv preprint arXiv:1605.09096*, 2016.
- Horace He and Thinking Machines Lab. Defeating nondeterminism in llm inference. *Thinking Machines Lab: Connectionism*, 2025. doi: 10.64434/tml.20250910. <https://thinkingmachines.ai/blog/defeating-nondeterminism-in-llm-inference/>.
- Ari Holtzman, Jan Buys, Li Du, Maxwell Forbes, and Yejin Choi. The curious case of neural text degeneration. *arXiv preprint arXiv:1904.09751*, 2019.
- Jenny Y Huang, Leshem Choshen, Ramon Astudillo, Tamara Broderick, and Jacob Andreas. Do llms benefit from their own words? *arXiv preprint arXiv:2602.24287*, 2026.
- Aaron Hurst, Adam Lerer, Adam P Goucher, Adam Perelman, Aditya Ramesh, Aidan Clark, AJ Ostrow, Akila Welihinda, Alan Hayes, Alec Radford, et al. Gpt-4o system card. *arXiv preprint arXiv:2410.21276*, 2024.
- Eric Jang, Shixiang Gu, and Ben Poole. Categorical reparameterization with gumbel-softmax. *arXiv preprint arXiv:1611.01144*, 2016.
- Albert Q Jiang, Alexandre Sablayrolles, Arthur Mensch, Chris Bamford, Devendra Singh Chaplot, Diego de las Casas, Florian Bressand, Gianna Lengyel, Guillaume Lample, Lucile Saulnier, et al. Mistral 7b. *arXiv preprint arXiv:2310.06825*, 2023.
- Liwei Jiang, Yuanjun Chai, Margaret Li, Mickel Liu, Raymond Fok, Nouha Dziri, Yulia Tsvetkov, Maarten Sap, Alon Albalak, and Yejin Choi. Artificial hivemind: The open-ended homogeneity of language models (and beyond). *arXiv preprint arXiv:2510.22954*, 2025.
- Florian Kandra, Vera Demberg, and Alexander Koller. Llms syntactically adapt their language use to their conversational partner. *arXiv preprint arXiv:2503.07457*, 2025.
- Simon Kirby, Mike Dowman, and Thomas L Griffiths. Innateness and culture in the evolution of language. *Proceedings of the National Academy of Sciences*, 104(12):5241–5245, 2007.
- Wojciech Kryściński, Nazneen Rajani, Divyansh Agarwal, Caiming Xiong, and Dragomir Radev. Booksum: A collection of datasets for long-form narrative summarization. In *Findings of the association for computational linguistics: EMNLP 2022*, pp. 6536–6558, 2022.
- Philippe Laban, Hiroaki Hayashi, Yingbo Zhou, and Jennifer Neville. Llms get lost in multi-turn conversation. *arXiv preprint arXiv:2505.06120*, 2025.
- Yubo Li, Xiaobin Shen, Xinyu Yao, Xueying Ding, Yidi Miao, Ramayya Krishnan, and Rema Padman. Beyond single-turn: A survey on multi-turn interactions with large language models. *arXiv preprint arXiv:2504.04717*, 2025.

- Yucheng Li, Frank Guerin, and Chenghua Lin. Latesteval: Addressing data contamination in language model evaluation through dynamic and time-sensitive test construction. In *Proceedings of the AAAI Conference on Artificial Intelligence*, volume 38, pp. 18600–18607, 2024.
- Erez Lieberman, Jean-Baptiste Michel, Joe Jackson, Tina Tang, and Martin A Nowak. Quantifying the evolutionary dynamics of language. *Nature*, 449(7163):713–716, 2007.
- Chin-Yew Lin. Rouge: A package for automatic evaluation of summaries. In *Text summarization branches out*, pp. 74–81, 2004.
- Nikolay Mikhaylovskiy. Zipf’s and heaps’ laws for tokens and llm-generated texts. In *Findings of the Association for Computational Linguistics: EMNLP 2025*, pp. 15469–15481, 2025.
- Amr Mohamed, Mingmeng Geng, Michalis Vazirgiannis, and Guokan Shang. Llm as a broken telephone: Iterative generation distorts information. In *Proceedings of the 63rd Annual Meeting of the Association for Computational Linguistics (Volume 1: Long Papers)*, pp. 7493–7509, 2025.
- Alberto Muñoz-Ortiz, Carlos Gómez-Rodríguez, and David Vilares. Contrasting linguistic patterns in human and llm-generated news text. *Artificial Intelligence Review*, 57(10):265, 2024.
- Vishakh Padmakumar and He He. Does writing with language models reduce content diversity? *arXiv preprint arXiv:2309.05196*, 2023.
- Kishore Papineni, Salim Roukos, Todd Ward, and Wei-Jing Zhu. Bleu: a method for automatic evaluation of machine translation. In *Proceedings of the 40th annual meeting of the Association for Computational Linguistics*, pp. 311–318, 2002.
- Jérémy Perez, Grgur Kovač, Corentin Léger, Cédric Colas, Gaia Molinaro, Maxime Derex, Pierre-Yves Oudeyer, and Clément Moulin-Frier. When llms play the telephone game: Cultural attractors as conceptual tools to evaluate llms in multi-turn settings. In *The Thirteenth International Conference on Learning Representations*, 2025.
- Andrew J Peterson. Ai and the problem of knowledge collapse. *AI & SOCIETY*, pp. 1–21, 2025.
- Rylan Schaeffer, Joshua Kazdan, Alvan Caleb Arulandu, and Sanmi Koyejo. Position: Model collapse does not mean what you think. *arXiv preprint arXiv:2503.03150*, 2025.
- Mohamed El Amine Seddik, Swei-Wen Chen, Soufiane Hayou, Pierre Youssef, and Merouane Debbah. How bad is training on synthetic data? a statistical analysis of language model collapse. *arXiv preprint arXiv:2404.05090*, 2024.
- Ilia Shumailov, Zakhar Shumaylov, Yiren Zhao, Nicolas Papernot, Ross Anderson, and Yarin Gal. Ai models collapse when trained on recursively generated data. *Nature*, 631(8022): 755–759, 2024.
- Brandon Smith, Mohamed Reda Bouadjeneq, Tahsin Alamgir Kheya, Phillip Dawson, and Sunil Aryal. A comprehensive analysis of large language model outputs: Similarity, diversity, and bias. *arXiv preprint arXiv:2505.09056*, 2025.
- Fengwei Teng, Quan Shi, Zhaoyang Yu, Jiayi Zhang, Yuyu Luo, Chenglin Wu, and Zhijiang Guo. Atom of thoughts for markov llm test-time scaling. *arXiv preprint arXiv:2502.12018*, 2025.
- Dustin Wright, Sarah Masud, Jared Moore, Srishti Yadav, Maria Antoniak, Peter Ebert Christensen, Chan Young Park, and Isabelle Augenstein. Epistemic diversity and knowledge collapse in large language models. *arXiv preprint arXiv:2510.04226*, 2025.

Weijia Xu, Nebojsa Jojic, Sudha Rao, Chris Brockett, and Bill Dolan. Echoes in ai: Quantifying lack of plot diversity in llm outputs. *Proceedings of the National Academy of Sciences*, 122 (35):e2504966122, 2025.

Hiromu Yakura, Ezequiel Lopez-Lopez, Levin Brinkmann, Ignacio Serna, Prateek Gupta, Ivan Soraperra, and Iyad Rahwan. Empirical evidence of large language model’s influence on human spoken communication. *arXiv preprint arXiv:2409.01754*, 2024.

An Yang, Baosong Yang, Binyuan Hui, Bo Zheng, Bowen Yu, Chang Zhou, Chengpeng Li, Chengyuan Li, Dayiheng Liu, Fei Huang, Guanting Dong, Haoran Wei, Huan Lin, Jialong Tang, Jialin Wang, Jian Yang, Jianhong Tu, Jianwei Zhang, Jianxin Ma, Jin Xu, Jingren Zhou, Jinze Bai, Jinzheng He, Junyang Lin, Kai Dang, Keming Lu, Keqin Chen, Kexin Yang, Mei Li, Mingfeng Xue, Na Ni, Pei Zhang, Peng Wang, Ru Peng, Rui Men, Ruize Gao, Runji Lin, Shijie Wang, Shuai Bai, Sinan Tan, Tianhang Zhu, Tianhao Li, Tianyu Liu, Wenbin Ge, Xiaodong Deng, Xiaohuan Zhou, Xingzhang Ren, Xinyu Zhang, Xipin Wei, Xuancheng Ren, Yang Fan, Yang Yao, Yichang Zhang, Yu Wan, Yunfei Chu, Yuqiong Liu, Zeyu Cui, Zhenru Zhang, and Zhihao Fan. Qwen2 technical report. *arXiv preprint arXiv:2407.10671*, 2024.

Oussama Zekri, Ambroise Odonnat, Abdelhakim Benechehab, Linus Bleistein, Nicolas Boullé, and Ievgen Redko. Large language models as markov chains. *arXiv preprint arXiv:2410.02724*, 2024.

A Token-level stochasticity and decoding

Iterative trajectories depend on decoding-induced stochasticity (Jang et al., 2016), in addition to system-level nondeterminism (He & Lab, 2025). At generation step t' , let $z(\cdot; x, w_{<t'})$ denote the logits given input x and prefix $w_{<t'}$. Temperature τ induces

$$\pi_\tau(w_{t'} | x, w_{<t'}) = \frac{\exp(z(w_{t'}; x, w_{<t'}) / \tau)}{\sum_v \exp(z(v; x, w_{<t'}) / \tau)}, \quad (12)$$

where larger τ typically increases randomness (Holtzman et al., 2019). Top- k , nucleus sampling (top- p), and logit controls further truncate or reweights this distribution (with limitations in some regimes (Chang & McCallum, 2022)). The probability of a length- n sequence is

$$\Pi_\tau(w_{1:n} | x) = \prod_{t'=1}^n \pi_\tau(w_{t'} | x, w_{<t'}). \quad (13)$$

These token-level choices induce the sentence-level transition kernel in Eq. (1) and can compound under iteration. Even when alternative decoding objectives are proposed, such as multi-token prediction (Gloeckle et al., 2024), the core stochastic selection mechanism remains central to typical deployments.

B Contraction of relative entropy

KL divergence is defined as,

$$D_{KL}(X \| Y) = \sum_i X_i \log \left(\frac{X_i}{Y_i} \right). \quad (14)$$

Similarly,

$$D_{KL}(X\mathbf{P} \| Y\mathbf{P}) = \sum_j (X\mathbf{P})_j \log \left(\frac{(X\mathbf{P})_j}{(Y\mathbf{P})_j} \right), \quad (15)$$

where $(X\mathbf{P})_j = \sum_i X_i P_{ij}$ and $(Y\mathbf{P})_j = \sum_i Y_i P_{ij}$. Assume $(Y\mathbf{P})_j > 0$ whenever $(X\mathbf{P})_j > 0$ (otherwise the divergence is infinite and the inequality holds trivially). By the log-sum inequality, for each j ,

$$\left(\sum_i X_i P_{ij} \right) \log \frac{\sum_i X_i P_{ij}}{\sum_i Y_i P_{ij}} \leq \sum_i X_i P_{ij} \log \frac{X_i P_{ij}}{Y_i P_{ij}}, \quad (16)$$

with the convention that terms with $X_i P_{ij} = 0$ contribute 0. Summing over j gives

$$D_{KL}(X\mathbf{P} \| Y\mathbf{P}) \leq \sum_j \sum_i X_i P_{ij} \log \frac{X_i P_{ij}}{Y_i P_{ij}} \quad (17)$$

$$= \sum_i X_i \log \frac{X_i}{Y_i} \sum_j P_{ij}. \quad (18)$$

Since \mathbf{P} is row-stochastic, $\sum_j P_{ij} = 1$, hence

$$D_{KL}(X\mathbf{P} \| Y\mathbf{P}) \leq D_{KL}(X \| Y). \quad (19)$$

C Prompts

This section lists the prompt templates used in the main experiments and ablations. In all listings, {content} is replaced with the current input text at iteration t , and {target_lang} denotes the chosen bridge language for round-trip translation. Unless stated otherwise, the same template is reused across iterations.

Tasks. Iterative rephrasing. Using rephrasing prompt ρ_{reph} , we iterate $s^{(t+1)} \sim \mathcal{T}_{M, \rho_{\text{reph}}, d}(\cdot | s^{(t)})$. **Iterated round-trip translation.** For bridge language ℓ with prompts ρ_{tr} , one iteration applies $\mathcal{T}_{M, \rho_{\text{tr}}, d}^{\text{EN} \rightarrow \ell \rightarrow \text{EN}}$ (Eq. 2):

$$s_{\text{EN}}^{(t)} \xrightarrow{\text{EN} \rightarrow \ell} u_{\ell}^{(t)} \xrightarrow{\ell \rightarrow \text{EN}} s_{\text{EN}}^{(t+1)}.$$

Rephrasing prompts. Listing 1 is the main meaning-preserving rephrasing template, and Listing 2 is a shorter ablation variant used in the prompt-sensitivity study.

Listing 1: Prompt for rephrasing

```
"Given a passage, rephrase it while preserving all the original
  meaning and without losing any context.\n"
"Do not write an introduction or a summary. Return only the rephrased
  passage.\n\n"
"Rephrase the following text:\n{content}"
```

Listing 2: Prompt for rephrasing (ablation)

```
"Rephrase the following text:\n{content}"
```

Translation prompts. For round-trip translation, we use direction-specific templates ($\text{EN} \rightarrow \ell$ and $\ell \rightarrow \text{EN}$). The current input text is appended after the instruction, and `{target_lang}` specifies the intermediate language ℓ .

Listing 3: Prompt for translation

```
"Translate the following English text into {target_lang}:"
"Translate the following {target_lang} text into English:"
```

D Additional Results

This section provides supplementary qualitative trajectories and full metric plots referenced in the main text. We include (i) iterative rephrasing examples under sampling, (ii) round-trip translation examples, (iii) similarity-metric trajectories for additional datasets/decoding regimes, and (iv) full length–diversity correlation outputs.

Iterative rephrasing under sampling. Table 3 shows representative trajectories under sampling-based decoding ($\tau = 0.7$, $\text{top-}p = 0.9$), illustrating how some chains exhibit continued drift while others still enter short cycles.

Iterated round-trip translation examples. Tables 4 and 5 provide illustrative round-trip translation chains ($\text{EN} \rightarrow \text{French} \rightarrow \text{EN}$), highlighting early stabilization and occasional alternation between near-identical variants.

Similarity dynamics across iterations. Figures 8 and 9 extend the greedy-decoding analysis to additional datasets. Figures 10–12 report the analogous plots under sampling-based decoding. As in the main text, each point compares iteration t to iteration $t - 1$ using METEOR, ROUGE-1, and BLEU.

Full length–diversity correlation results. Table 6 reports Pearson correlations between seed length and diversity, along with p -values, linear-fit R^2 , and slopes for each model/decoding setting and dataset.

Round	Llama-3.1-8B-Instruct	Qwen2.5-7B-Instruct
0	We begin with a prologue.	We begin with a prologue.
1	The narrative commences with a prologue.	We start with a prologue.
2	The story begins with a prologue that sets the scene.	We begin with a prologue.
3	The narrative commences with a prologue that establishes the backdrop for the story.	We start with a prologue.
5	The story starts with a prologue, which establishes the setting and lays the groundwork for the events that unfold in the narrative.	We start with a prologue.
10	The narrative begins with a prologue, which sets the scene and lays the groundwork for the events that unfold in the story that follows.	We begin with a prologue.
20	The narrative begins with a prologue, establishing the groundwork and setting the scene for the events that will unfold throughout the story.	We begin with a prologue.
30	The narrative begins with a prologue that sets the scene and lays the groundwork, providing a solid foundation for the events that follow to unfold and develop.	We begin with a prologue.
40	The narrative begins with a prologue that sets the scene, provides essential background information, and lays the groundwork, establishing a solid foundation that allows the subsequent events to unfold in a logical and cohesive manner.	We begin with a prologue.
49	The story starts with a prologue that lays the groundwork by providing key background information and establishing the setting, thus creating a solid foundation that allows the subsequent events to unfold in a logical and coherent manner.	We start with a prologue.
50	The story begins with a prologue that sets the stage by offering essential background information and establishing the setting, thereby laying a solid foundation that enables subsequent events to unfold in a logical and coherent way.	We begin with a prologue.

Table 3: Examples of repeated rephrasing by different LLMs (temperature=0.7, top-p=0.9).

Round	French	English
0		We begin with a prologue.
1	Nous commençons par un prologue.	We begin with a prologue.
2	Nous commençons par un prologue.	We begin with a prologue.
3	Nous commençons par un prologue.	We begin with a prologue.
4	Nous commençons par un prologue.	We begin with a prologue.

Table 4: Examples of iterative translation via GPT-4o-mini (temperature=0.7, top-p=0.9).

Round	French	English
0		Elizabeth reads through Darcy’s letter with a mixture of emotions.
1	Elizabeth lit la lettre de Darcy avec un mélange d’émotions.	Elizabeth read Darcy’s letter with a mix of emotions.
2	<i>Elizabeth a lu la lettre de Darcy avec un mélange d’émotions.</i>	<i>Elizabeth read Darcy’s letter with a mix of emotions.</i>
⋮	⋮	⋮
11	Elizabeth lut la lettre de Darcy avec un mélange d’émotions.	Elizabeth read Darcy’s letter with a mixture of emotions.
12	Elizabeth a lu la lettre de Darcy avec un mélange d’émotions.	Elizabeth read Darcy’s letter with a mixture of emotions.
⋮	⋮	⋮
19	Elizabeth lut la lettre de Darcy avec un mélange d’émotions.	Elizabeth read Darcy’s letter with a mix of emotions.

Table 5: Examples of iterative translation via GPT-4o-mini (temperature=0.7, top-p=0.9). The omitted lines are all identical to the content in the second round (the italicized sentences). The similar scenario also occurs after the 19th round.

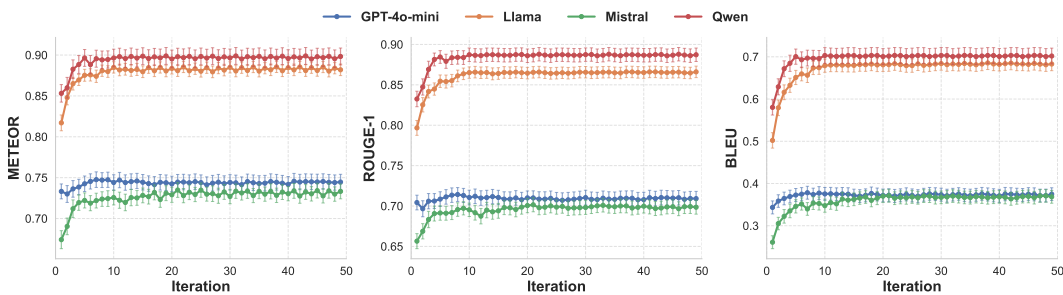


Figure 8: Evolution of text similarity metrics across 50 rephrasing iterations for the News2024 dataset using greedy decoding. Each iteration compares the current rephrased text against the previous iteration’s text as reference.

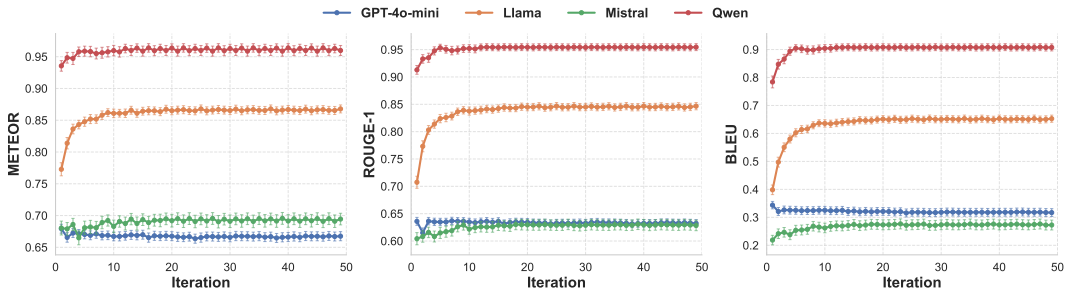


Figure 9: Evolution of text similarity metrics across 50 rephrasing iterations for the ScriptBase dataset using greedy decoding. Each iteration compares the current rephrased text against the previous iteration’s text as reference.

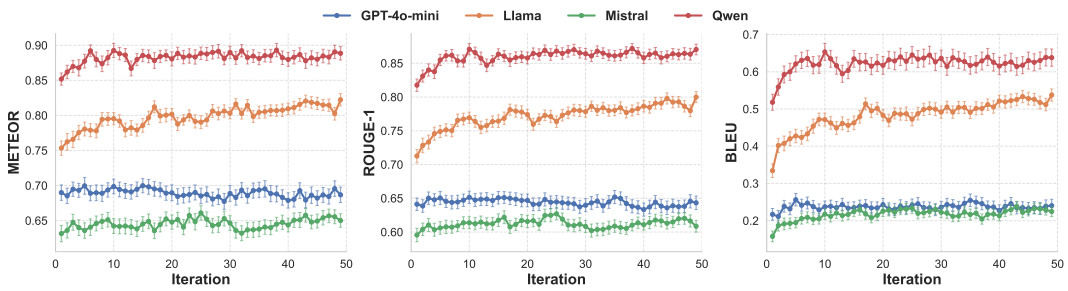


Figure 10: Evolution of text similarity metrics across 50 rephrasing iterations for the BookSum dataset using sampling-based decoding. Each iteration compares the current rephrased text against the previous iteration’s text as reference.

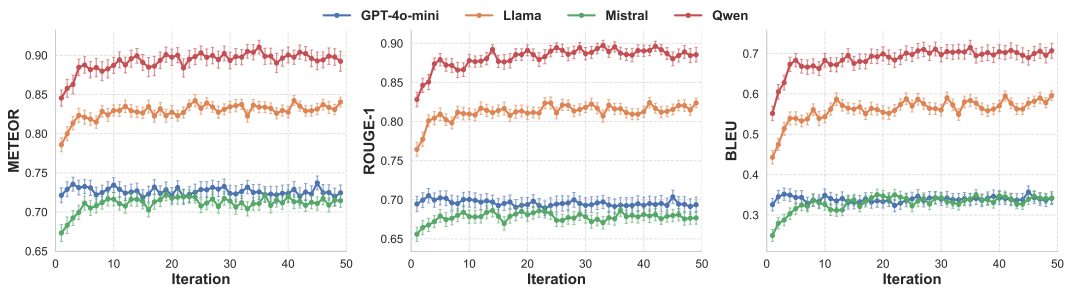


Figure 11: Evolution of text similarity metrics across 50 rephrasing iterations for the News2024 dataset using sampling-based decoding. Each iteration compares the current rephrased text against the previous iteration’s text as reference.

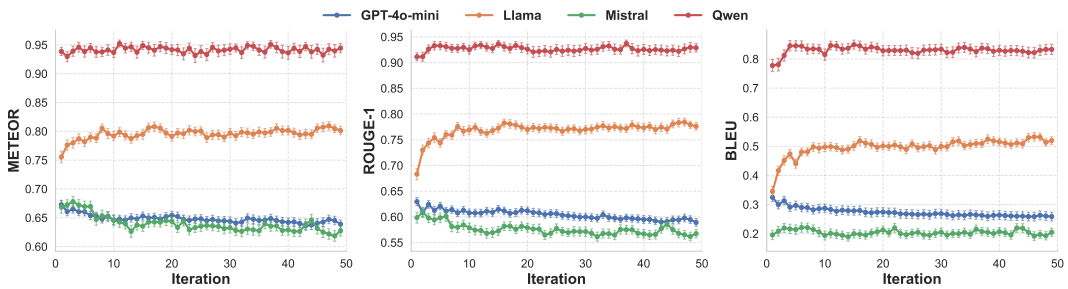


Figure 12: Evolution of text similarity metrics across 50 rephrasing iterations for the Script-Base dataset using sampling-based decoding. Each iteration compares the current rephrased text against the previous iteration’s text as reference.

Dataset	Model	r	p	R ²	Slope
booksum	Llama greedy	0.171	3.611e-02	0.029	0.107
	Llama sample	0.166	4.272e-02	0.027	0.191
	Mistral greedy	0.324	5.135e-05	0.105	0.350
	Mistral sample	0.438	2.046e-08	0.192	0.594
	Qwen greedy	0.353	9.427e-06	0.125	0.125
	Qwen sample	0.494	1.330e-10	0.244	0.616
	GPT greedy	0.476	7.658e-10	0.226	0.261
	GPT sample	0.638	1.542e-18	0.407	1.054
scriptbase	Llama greedy	-0.174	3.338e-02	0.030	-0.238
	Llama sample	0.030	7.150e-01	0.001	0.048
	Mistral greedy	0.073	3.731e-01	0.005	0.124
	Mistral sample	-0.021	8.012e-01	0.000	-0.050
	Qwen greedy	0.094	2.510e-01	0.009	0.056
	Qwen sample	0.157	5.479e-02	0.025	0.272
	GPT greedy	0.105	2.017e-01	0.011	0.109
	GPT sample	0.231	4.471e-03	0.053	0.727
news2024	Llama greedy	0.187	2.216e-02	0.035	0.107
	Llama sample	0.114	1.659e-01	0.013	0.081
	Mistral greedy	0.111	1.757e-01	0.012	0.118
	Mistral sample	0.197	1.585e-02	0.039	0.141
	Qwen greedy	0.199	1.454e-02	0.040	0.058
	Qwen sample	0.373	2.600e-06	0.139	0.477
	GPT greedy	0.367	3.765e-06	0.135	0.203
	GPT sample	0.385	1.116e-06	0.149	0.525

Table 6: Results of the Correlation Analysis. r represents the Pearson correlation coefficient, and R^2 represents the coefficient of determination.